Study of the Affinity of Thermographic Additives for Silver by Time-of-Flight Static Secondary Ion Mass Spectrometry and Surface-Enhanced Raman Spectroscopy on Silver Nanoparticles

Roel De Mondt,*,† Kitty Baert,‡ Ingrid Geuens,§ Luc Van Vaeck,† and Annick Hubin‡

Department of Chemistry, University of Antwerp, Universiteitsplein 1, 2610 Wilrijk, Belgium, Department of Metallurgy, Electrochemistry and Materials Science, Vrije Universiteit Brussel (VUB), 1050 Brussel, Belgium, and Agfa-Gevaert N.V., Septestraat 27, 2640 Mortsel, Belgium

Received June 2, 2006. In Final Form: September 28, 2006

Detection of the interactions between low molecular weight organic compounds and metals in the form of sols on a nanoscale is analytically challenging. This study aims to provide experimental evidence using a combination of UV−Vis absorption spectrometry, surface-enhanced Raman spectrometry (SERS), and static secondary ion mass spectrometry (S-SIMS). The field of application is thermography where silver images are formed via heat-catalyzed reactions. Several organic compounds called tone modifiers and stabilizers are used in thermographic materials for the optimization of the image quality. With exploitation of the strengths of each of the above-mentioned methods, an affinity ranking of several tone modifiers and a stabilizer was established on the basis of competitive adsorption experiments using different model systems. Specifically, silver sols, SERS probes, and sputter-coated silver substrates were exposed to systems with one or two additives. The UV−Vis results provided insight on the aggregation of silver nanoparticles in a hydrosol, which was necessary for the interpretation of the SERS data. Both SERS and S-SIMS measurements led to a similar ranking of the relative affinity of the additives in two components, which was largely consistent with empirical knowledge derived from macroscopic behavior.

1. Introduction

Thermographic materials can be found in everyday life as digital hardcopy images of medical radiographs. In general, thermography generates images by heating the recording material, which contains compounds that irreversibly change color or optical density by chemical or physical processes. Most of the "direct" thermographic recording materials (as opposed to photothermography) are of the chemical type.[1−4] Such a thermographic film consists of (substantially light-insensitive) organic silver salts, reducing agents, tone modifiers, and stabilizers, embedded in a polymeric layer. The heat-catalyzed reduction of Ag^+ from the organic salt to Ag^0 is responsible for image formation.

During the thermal development process the reducing agent must be able to diffuse to the particles of the organic silver salt so that reduction to Ag^0 can occur. The tone modifiers must exhibit good silver nanoparticle-aggregating properties. Stabilizers are present to preserve the image quality. Since thermographic recording materials contain the imaging-forming components after image formation, subsequent transformation during storage and upon exposure to light must be avoided. There is therefore a need for stabilizing compounds.

The performance of a thermographic system depends on the physicochemical interaction between the organic additives and the silver component. Stabilizers and tone modifiers should, for example, work at specific moments of the product processing. The affinity of each additive toward the various forms of silver (organic salt as well as metallic silver) is crucial for the performance and behavior of the thermographic material in processing, storing, and handling.

Even today, the constituents of the thermographic film are primarily selected in an empirical way. The formulation of a thermographic film is changed and macroscopic properties such as color density as a function of heating intensity and duration are measured to define and verify hypotheses. This has yielded a rough idea about the reactivity of some components toward each other and toward silver and organic silver salts.

The purpose of this study is to extend our insight in the local interactions and functional properties of the components of the thermographic material (Ag^0 + toning agents + stabilizers), present in discrete phases on a nanoscale. Specifically, the relative affinity between the components and the silver is of interest as it defines the surface coverage of the discrete silver phases in multicomponent systems. At this moment, no single analytical method allows a full description of the chemical composition in terms of molecular information from complex systems on a nanoscale. Therefore, this study has been based on the complementary use of different analysis techniques, applied to simplified model systems that mimic the interactions in the real material. Specifically, UV−Vis spectrometry, Raman spectrometry, SERS, and S-SIMS have been applied to samples consisting of silver in nanometer-scale hydrosol or deposited on a dedicated SERS probe, as well as on silver sputter-coated substrates exposed to solutions of the individual components or mixtures.

The choice of the analytical methods has been motivated by their complementary characteristics with respect to the information required. The use of UV−Vis spectrometry provides information about the interaction of light with particles of different sizes. A silver colloid is used as a model system. The information

* To whom correspondence should be addressed. E-mail: roel.demondt@ua.ac.be. Tel.: +32 3 820 2389. Fax: +32 3 820 2376.

† University of Antwerp.

‡ Vrije Universiteit Brussel.

§ Agfa-Gevaert N.V.

(1) Geuens I.; Vanwelkenhuysen I. *J. Imag. Sci. Technol.* **1999**, *43* (6), 521−527.

(2) Patent, EP848286. Thermographic recording material with improved image tone and/or stability upon thermal development.

(3) Patent, EP1431814. Toning agents for use in substantially light-insensitive recording materials.

(4) Patent, US2005136363. Stabilizers for use in thermographic recording materials.

10.1021/la061591v CCC: $33.50
Published on Web 11/15/2006

obtained is the size of the silver particles in the colloid solution[5] and more specifically the degree of aggregation of the silver particles due to the organic additives. A second approach uses Raman spectrometry. This technique detects the formation of complexes between the organic additives and the silver by measuring changes in the vibrational energies of the molecules. The well-known SERS effect (enhancement of Raman signal intensities) occurs on noble metals and can be exploited in these experiments since silver is of particular interest. The SER spectra reflect the Ag-substrate−adsorbate interactions and thereby allow the adsorption behavior of the organic molecules on silver to be studied.[6−10] When the method is applied to the colloidal systems mentioned above, the adsorption of organic additives and the competition between individual components can be investigated. Based on these data, an affinity ranking of the additives can be created, which is an essential property for the optimization of thermographic materials. Moreover, use of a newly developed measuring technique allows SERS to be performed on a probe consisting of silver nanoparticles in gelatin on which a drop of a solution with one or more additives is deposited.

Finally, S-SIMS has been used because it can provide molecular information on the components in essentially the uppermost monolayer on a given surface. The surface is bombarded with primary ions and the secondary ions generated from the surface are detected as a function of their mass-to-charge ratio (m/z).[11] The application of a limited primary ion dose density in the so-called static regime (cf. Experimental Section) allows S-SIMS to detect structural ions from the sample. In this study, S-SIMS has been used for the analysis of samples consisting of adsorbed layers of thermographically active compounds on silver surfaces. The specific interest in the interactions between organic additives and silver benefits from the well-known enhancement of the secondary ion yields from thin films of organic compounds on noble metals.[12−14] In comparison to SERS, which essentially characterizes the strength of individual bonds, S-SIMS provides the advantage of full molecular information, i.e., the molecular weight (MW) of the (interaction) product as well as structural information via the specific fragments. Besides the structural insight in the interaction products, quantitative use of the peak intensities allows the ranking of different components according to their affinity for silver to be established independently from SERS, using exposure of the substrate to multicomponent solutions.

2. Experimental Section

2.1. Reagents. All chemicals were provided by Agfa-Gevaert (Mortsel, Belgium). The molecular structures and abbreviations are shown in Figure 1. All are tone modifiers except 1*H*-1,2,3-benzotriazole (BZTR) which is a stabilizer. Solutions for the SERS and UV experiments were prepared in methanol (10^{-2} M) and further diluted to 5×10^{-4} to 10^{-4} M with deionized water. For the S-SIMS experiments, solutions were prepared in 2-butanone (10^{-2} M) (99+%, Acros, Geel, Belgium).

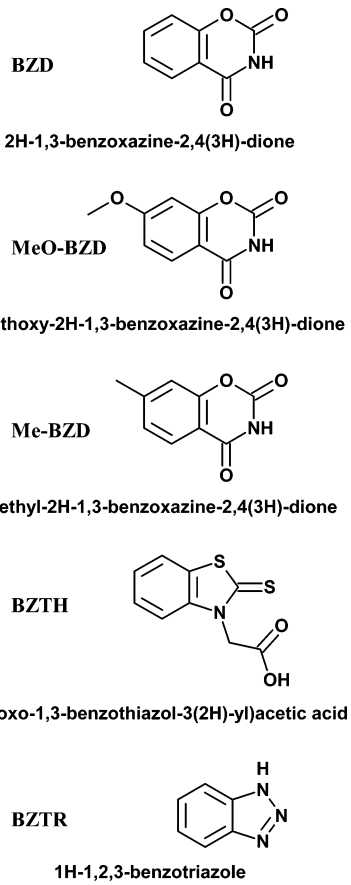

Figure 1. Molecular structures and abbreviations of the studied compounds. All are tone modifiers except BZTR, which is a stabilizer.

2.2. Silver Colloid Samples for UV−Vis and SERS. A silver sol was prepared by adding 50 mL of 2×10^{-3} M $AgNO_3$ dropwise to 150 mL of 2×10^{-3} M KBH_4 (p.a., Fluka, Buchs, Switzerland). The resulting colloidal solution was yellow (Ag particles of 5−20 nm). An aliquot of 0.5 mL of the additive solution was added to 5 mL of silver sol (final concentration 10^{-5} to 5×10^{-5} M, i.e., approximately 100% surface coverage, without excess).[15] For each solution, the aggregation process was stopped after 10 s by adding 5 mL of a 0.5% gelatin solution in water. The pH of the solutions (sol + additives) had a constant value of 8.5.

2.3. SERS Probe Samples. Beside the silver sol, a SERS probe, developed in-house at the Vrije Universiteit Brussel, was also used as a substrate for SERS measurements. It consisted of silver particles in a gelatin matrix on a glass substrate (76 × 26 mm), ensuring a good SERS enhancement.[3,16,17] Adsorption phenomena occurring in the silver sol were monitored using this tool. Therefore, a droplet of tone modifier solution with a concentration of 5×10^{-5} M was spotted on the probe surface. In this way, SER spectra could be recorded directly.

2.4. Samples for S-SIMS Analysis. Thin layers of additives were prepared by dip coating Ag-covered Si wafers in compound solutions. The Si wafers were test grade silicon (14.5−20 Ω-cm, Montco Silicon, Spring City, PA). They were thoroughly cleaned by 10 min of sonification in methanol and dried in a stream of hot air. Coating

(5) Creighton, J. A.; Blatchford, C. G.; Albrecht, M. G. *J. Chem. Soc., Faraday Trans. 2* **1979**, *75*, 790−798.
(6) Creighton, J. A. In *Surface Enhanced Raman Spectroscopy*; Chang, R. K., Furtak, T. E., Eds.; Plenum Press: New York, 1982; p 315.
(7) Gonnissen, D.; Hubin, A.; Vereecken, J. *Electrochim. Acta* **1999**, *44* (24), 4129−4137.
(8) Gonnissen, D.; Langenaeker, W.; Hubin, A.; Geerlings, P. *J. Raman Spectrosc.* **1998**, *29* (12), 1031−1039.
(9) Tielens, F.; Saeys, M.; Tourwe, E.; Marin, G. B.; Hubin, A.; Geerlings, P. *J. Phys. Chem. A* **2002**, *106* (7), 1450−1457.
(10) Tourwe, E.; Baert, K.; Hubin, A. *Vib. Spectrosc.* **2006**, *40* (1), 25−32.
(11) Van Vaeck, L.; Adriaens, A.; Gijbels, R. *Mass Spectrom. Rev.* **1999**, *18*, 1−47.
(12) Lange, W.; Jirikowsky, M.; Benninghoven, A. *Surf. Sci.* **1984**, *136* (2−3), 419−436.
(13) Rüschenschmidt, K.; Schnieders, A.; Benninghoven, A.; Arlinghaus, H. F. *Surf. Sci.* **2003**, *526* (3), 351−355.
(14) Hagenhoff, B. Noble metal supports in organic SIMS. In *The Static SIMS Library*; SurfaceSpectra Ltd: Manchester, 1998; pp 39−46.
(15) Joo, S. W.; Han, S. W.; Kim, K. *J. Colloid Interface Sci.* **2001**, *240*, 391−399.
(16) Patent, EP1435298. Toning agents for use in thermographic and photothermographic recording materials.
(17) Tourwe, E.; Hubin, A.; Gonnissen, D. *Proceedings of the International Symposium on Progress in Surface Raman Spectroscopy − Theory, Techniques & Applications*; Tian, Z. Q., Ren, B., Eds.; Xiamen University Press: Xiamen, China, 2000; pp 71−72.

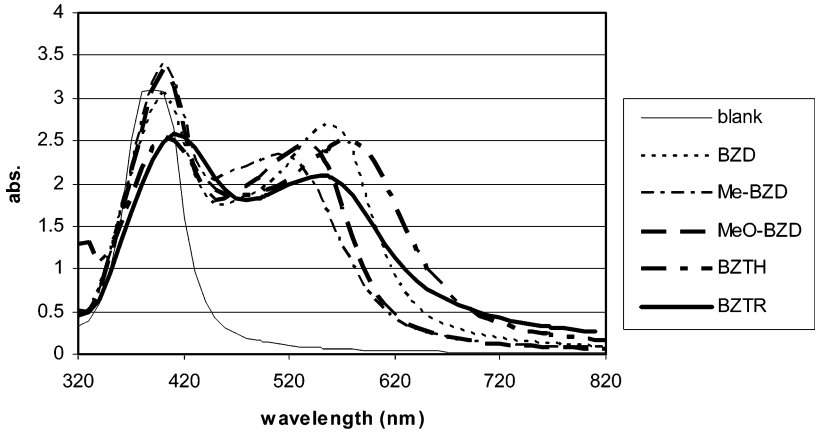

Figure 2. Overlay of UV−Vis absorption spectra of silver hydrosols exposed to solutions without and with one additive.

the Si wafers with Ag was carried out for 300 s in a Bal-Tec (Balzers, Liechtenstein) sputter coater SCD 005 at an Ar pressure of 0.05 mbar and a current of 60 mA. The estimated layer thickness of about 70 nm is well above the information depth of S-SIMS. The use of sputter-coated Ag on Si instead of the more easily prepared etched Ag substrates was motivated by the more homogeneous ion yield from evaporated Ag substrates.[18] Adsorption was performed by exposing Si wafers for 1 h in the above-mentioned solutions. Both the single-component and the multicomponent solutions contained the particular additives at a concentration of 0.01 M. Subsequently, the wafers were immediately washed by dipping them in water and drying them in a stream of hot air. The wafers were kept horizontal when moving them in and out of solutions to prevent trickling and ensure repeatability of the sample preparation.

2.5. Instrumentation. The UV−Vis spectra were recorded with a HP8452A Diode Array spectrophotometer (Hewlett-Packard, Palo Alto, CA) with a 2 nm wavelength resolution and 1 s integration time.

The SER spectra were obtained on a DILOR XY spectrometer (HORIBA Jobin Yvon Inc, Edison, NJ), equipped with an Olympus (Olympus, Tokyo, Japan) H2 microscope (magnification of 50×, focal length of 8 mm), a single monochromator, a notch filter, and a liquid nitrogen cooled charge-coupled device detector with resolution of ∼2 cm^{-1}. Excitation was provided by the 514 nm radiation of a Coherent Innova 70C Argon/Krypton mixed gas laser (Coherent Inc., Santa Clara, CA). The output power and acquisition time were 50 mW and 30 s, respectively, for liquid sol samples, while values of 10 s and 20 mW were used for the solutions on the probe and 30 s and 12 mW for the dry samples. The measured Raman intensities are a function of these settings and are not shown in the figures. Therefore, only the spectra obtained at similar conditions are grouped in one figure and are shown in a stacked display mode. The background signal is subtracted and the spectra are normalized to the most intense peak.

The TOF-S-SIMS experiments were carried out with an Ion TOF IV instrument (Ion ToF, Muenster, Germany). A liquid metal ion gun was used to generate 25 keV Ga^+ primary ions using a dc current of 1.3 nA and pulse width of 30 ns bunched down to ∼1 ns at a repetition rate of 10 kHz. Positive ion mass spectra in the range of m/z 1−850 were acquired from 100 × 100 μm^2 areas over 200 s, resulting in a total ion dose density of 3.7×10^{12} ions cm^{-2}, which is below the generally accepted static limit of below 10^{13} ions cm^{-2}.

The static regime in S-SIMS can be explained as follows. As the impact of a primary ion destroys the molecular structures in the sample over a given area (typically 10 nm^2) around the point of impact, detection of molecular information implies that no spot should be hit twice. The static limit refers to the maximum allowable ion dose density that makes less than 1% of the surface area inadequate for further analysis. A full discussion is given elsewhere.[11]

Positive ion mass spectra were calibrated using the signals for H^+, CH_3^+, $C_2H_5^+$, $C_3H_7^+$, and $C_4H_9^+$ at m/z 1, 15, 29, 43, and 57, respectively. Integration of the peak areas by IonSpec was used to calculate the ion intensities. Every sample was analyzed three times.

3. Results and Discussion

The same sample composition was prepared for SERS hydrosol analysis as for S-SIMS and UV−Vis spectrometry. One-component solutions as well as two-component solutions were prepared. In the SERS and S-SIMS measurements these two kinds of samples were compared to monitor the influence of one compound on the other. All combinations of tone modifiers with one another and with the stabilizer were tested.

3.1. Aggregation of Silver through Adsorption of Additives. *3.1.1. One-Component Solutions.* When the additives are added to the silver sol, the sol color changes immediately from yellow to red/purple due to colloid aggregation.[19] Figure 2 shows that the UV−Vis absorption spectra of the solution containing an additive exhibit a second absorption maximum in the wavelength range 520−620 nm, complementing the absorption at ∼400 nm.

The second absorption maximum for the solutions with BZD, Me−BZD, MeO−BZD, or BZTH results in a bright sol with a specific pure color. The shift of this absorption maximum is caused by an increase in the degree of aggregation,[5] which in turn depends on the presence of the additive. The activity of the additives in this respect can be ranked according to the order BZTH (λ_{max} at 580 nm) > BZD (λ_{max} at 560 nm) > MeO−BZD (λ_{max} at 530 nm) > Me−BZD (λ_{max} at 510 nm). The color of the sol with BZTR is less bright (red-brown) and this correlates with the broader absorption band compared to those of the tone modifiers. The λ_{max} occurs at 555 nm and there is a tail on the long-wavelength side, which indicates a larger range of colloid sizes.

3.1.2. Two-Component Solutions. If two additives are added together to the silver sol, one compound always dominates the aggregation process. The absorption spectra of the sol exposed to a combination of tone modifiers can be found in Figure A of the Supporting Information. The mixtures with BZTH consistently exhibit a higher degree of aggregation (maximum absorption at ∼570 nm) comparable with the pure BZTH solution (see Figure 2). Although Me−BZD alone gives less aggregation than the other tone modifiers in the silver sol, it plays an important role in the aggregation process when combined with BZD and MeO−BZD. The maximum absorption always occurs at 530 nm and the absorbance is similar to that of Me−BZD alone.

(18) De Mondt, R.; Van Vaeck, L.; Lenaerts, J.; Geuens, I.; Van Luppen, J. *Rapid Commun. Mass Spectrom.* **2006**, *20*, 641−652.

(19) Montes, R.; Contreras, C.; Rupérez, A.; Laserna, J. J. *Anal. Chem.* **1992**, *64*, 2715−2719.

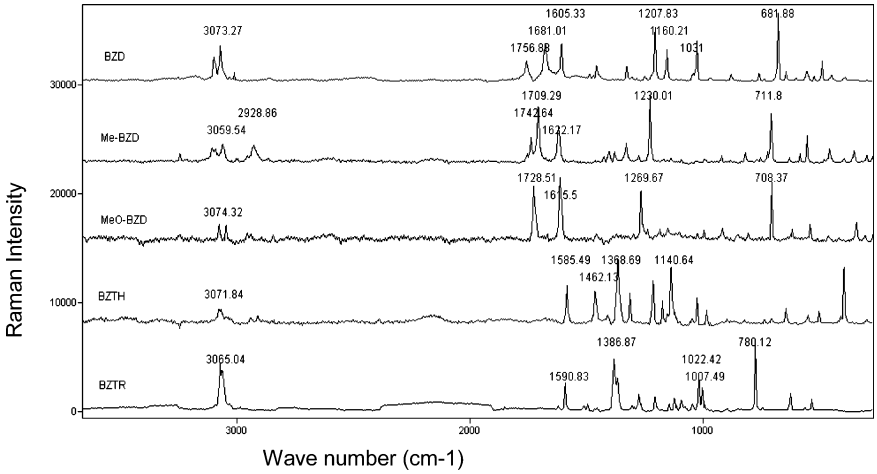

Figure 3. Normal Raman (NR) spectra of BZD, Me−BZD, MeO−BZD, BZTH, and BZTR in the solid state.

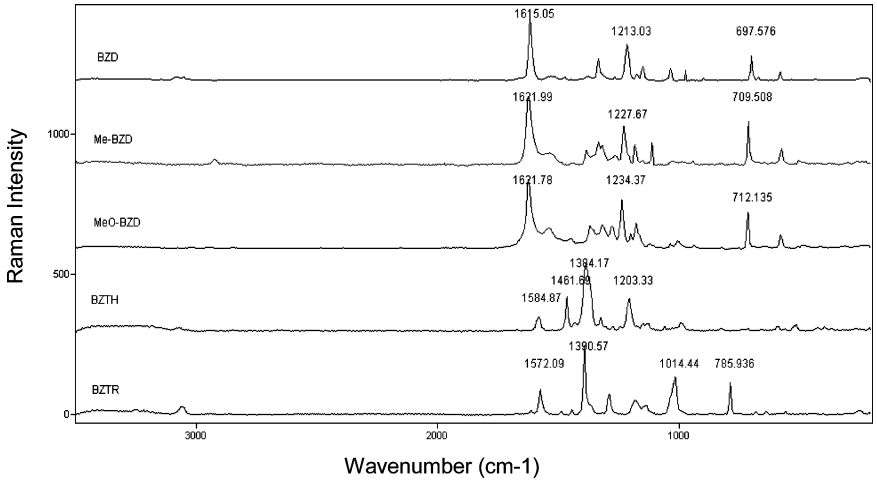

Figure 4. SER spectra of BZD, Me−BZD, MeO−BZD, BZTH, and BZTR on a Ag sol.

The absorption spectra of the sol exposed to combinations of the stabilizer BZTR with each of the four tone modifiers are shown in Figure B of the Supporting Information. There is no longer a well-defined absorption maximum at higher wavelengths. Hence, the aggregation process gives a higher distribution of the aggregates. This phenomenon is more pronounced with BZTH, which alone in the solution gives the highest (uniform) degree of aggregation (see Figure 2). Based on these observations, it can be concluded that the order of domination in the aggregation process is as follows: BZTR > BZTH > Me−BZD > MeO−BZD = BZD. Note that the phenomena observed in the silver sol also occur for tone modifier concentrations of 10^{-3} M (excess of ~100×). At lower concentrations (<5×10^{-6} M, less than 100% surface coverage) the aggregation is limited and at a concentration of 10^{-6} M tone modifier there is no aggregation (results not shown).

3.2. Relative Affinity Using SERS. Within the framework of this study, the features of Raman spectra taken from additive solutions mixed with silver sols potentially represent an interesting way to get information on the interaction between the additive and the silver sol. The reason is that the SERS effect implies a close bonding of the analyte and the noble metal surface.[7,8] The feasibility of this approach has been demonstrated by using the SER spectrum of each molecule as a "fingerprint". Clues about the affinity ranking process were sought from a comparison of the SER spectra with these characteristic fingerprints.

The normal Raman (NR) spectra of the five compounds in the solid state and the SER spectra of the compounds in the Ag hydrosol solution are shown in Figures3 and 4, respectively.

Table 1. Survey of the Most Characteristic SERS Bands for the Different Additives

compound	wavenumber (cm^{-1}) of characteristic bands		
BZD	1615	1213	697
Me−BZD	1622	1228	709
MeO−BZD	1622	1234	712
BZTH	1585	1461	1384
BZTR	1572	1390	786

A comparison between the SER and the NR spectra shows great similarities, but also differences in the wavenumber and intensity of the vibrational bands. From these data it is clear the measured Raman signal in the silver sol is a SER spectrum because (i) the positions of some of the bands are shifted due to the coupling of the Ag plasmon to the organic and (ii) the compounds cannot be measured at these concentrations (10^{-5} M) using normal Raman with no enhancement. This enhancement depends on the size of the silver colloid.[20] However, because the second maximum in the UV−Vis absorption spectra is found in the same region of 510−580 nm for all compounds, it is assumed that the aggregation is similar and that the surface enhancement effect is similar. The measured intensities of the SER spectra in Figure 4 are of similar magnitude.

Table 1 gives the wavenumbers of the signals that have been selected from the SERS fingerprints to characterize the additives.

(20) Brolo, A. G.; Irish, D. E.; Szymanski, G.; Lipkowski, J. *Langmuir* **1998**, *14*, 517−527.

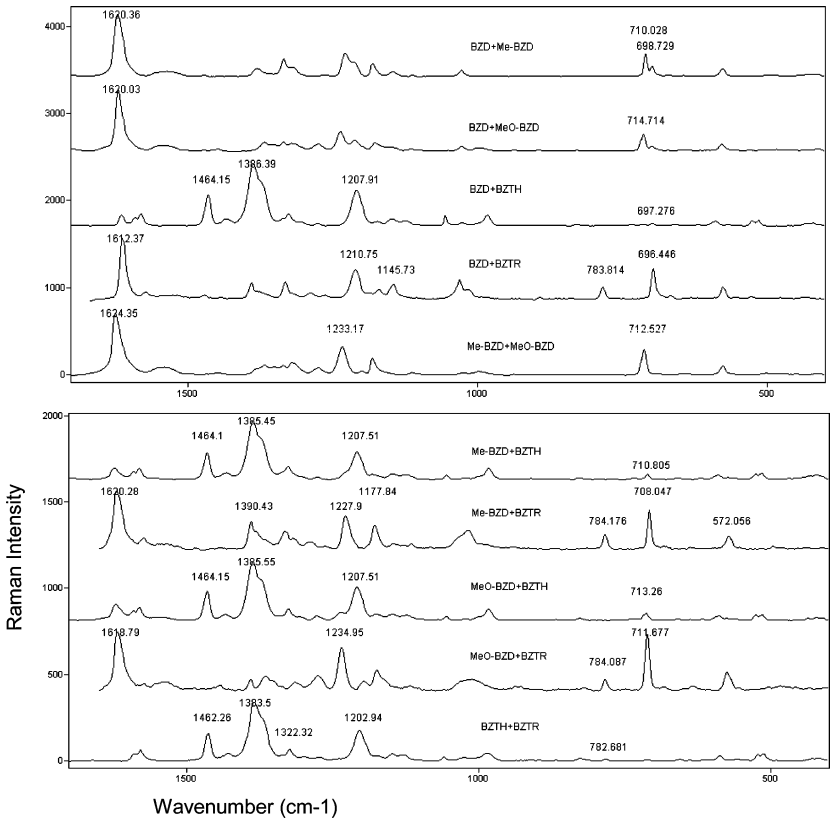

Figure 5. SER spectra from Ag sols exposed to the different two-component mixtures.

The vibrational spectrum of BZD is rather complicated and there is very little information in the literature to support the assignment.[21] The band at ∼1750 cm^{-1} of the carbonyl groups (C═O vibrations) is absent in the SERS mode and also the bands at higher wavenumbers (3050−3100 cm^{-1}, CH stretching) become very weak. The most enhanced bands, at 1615 cm^{-1} (aromatic ring stretch), 1213 cm^{-1} (in-plane ring stretch), and 697 cm^{-1} (most probably ring breathing), were used to track BZD. The spectra of Me−BZD and MeO−BZD, especially in SERS, were similar. The shift to higher wavelengths in the SERS mode permitted the adsorptions of the different molecules to be distinguished.

By comparison of the spectra of BZTH with NR/SERS results of similar molecules in the literature,[22] some important bands can be assigned, i.e., 1585 cm^{-1} (NR and SERS, ring stretching), 1461 cm^{-1} (NR═SERS, ring stretching/in-plane bending), and 1368 cm^{-1} in NR and 1384 cm^{-1} in SERS (ring stretching of C−N). For BZTR, three bands could be used as guiding spectral lines,[23] namely, 780 cm^{-1} in NR and 786 cm^{-1} in SERS (in-plane-bending of benzene ring), 1386 cm^{-1} in NR and 1390 cm^{-1} in SERS (triazole ring stretching), and 1590 cm^{-1} in NR and 1572 cm^{-1} in SERS (CC stretching). As the most important bands for each compound were found between 600 and 1700 cm^{-1}, the SERS measurements on the Ag sol exposed to two components were confined to this range. Figure 5 shows the results of all combinations.

A strictly quantitative interpretation of the spectra is beyond the scope of this feasibility study. The relative importance of the contribution from different additives to the SER spectra was taken as a measure for the amount of adsorbed molecules. This is based on the observation that all additives yield signals with comparable intensities in the one-component solutions.

For the four combinations with BZD, the intensity of the characteristic bands (e.g., at 697 cm^{-1}) of this compound was always weaker than that for the peaks from the other compounds. The signals at peaks at 710 and 714 cm^{-1} suggest that the affinity to silver is comparable for Me−BZD and MeO−BZD and is obviously stronger than that of BZD. In mixtures with BZTH, the contribution in the SER spectra of other additives was limited. The behavior of BZTR was little different. As seen for the other compounds, there is almost no co-adsorption with BZTH, but a comparison of the peak intensities at 784 cm^{-1} (BZTR) and 697, 708, or 712 cm^{-1} (tone modifiers) shows that there is always a significant co-adsorption with BZD, Me−BZD, and MeO−BZD.

The results obtained with SERS for the different solutions and the assumptions made according to their interpretation lead to the following order of Ag affinity within the group of tone modifiers: BZTH ≫ Me−BZD = MeO−BZD > BZD. The presence of the stabilizer BZTR in the two-component mixture removed the distinction in affinity between BZD and the two other variants. However, there is much more adsorption of BZTH in comparison to adsorption of all BZTR. Therefore, a total affinity scale should rank BZTR between BZTH and the BZD variants.

Finally, to assess the reproducibility of these results in different SERS analysis conditions, an aqueous solution containing one or two additives was applied to the SERS probe developed at the VUB.[3,16] These results are provided in Figure C of the Supporting Information. The relative contribution from the different components in solution was used in the same way as described before, to assess the Ag affinity. The experiments yielded the same order, namely, BZTH ≫ Me−BZD = MeO−BZD > BZD. In these experiments a clearer insight was obtained

(21) Dunkers, J.; Ishida, H. *Spectrochim. Acta* **1995**, *51A* (6), 1061−1074.
(22) Pergolese, B.; Bigotto, A. *J. Raman Spectrosc.* **2003**, *34*, 84−89.
(23) Metikoš-Huković, M.; Furić, K.; Babić, R.; Marinović, A. *Surf. Interface Anal.* **1999**, *27*, 1016−1025.

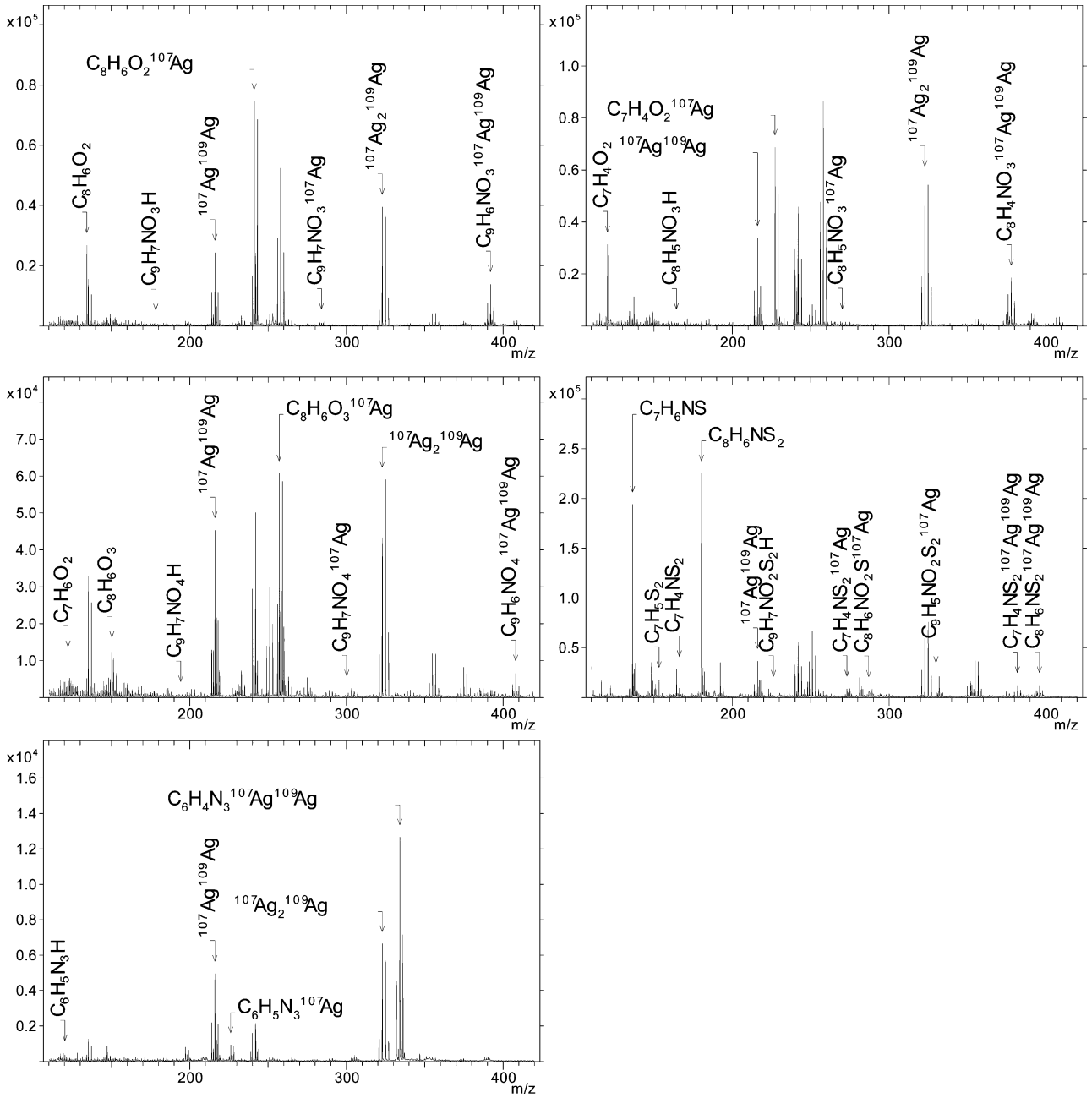

Figure 6. Positive ion secondary ion mass spectra of dip-coated compounds on evaporated Ag: upper left, Me−BZD; upper right, BZD; middle left, MeO−BZD; middle right, BZTH; bottom left, BZTR.

on the stronger affinity of BZTR as opposed to those of BZD and derivatives thereof.

3.3. Relative Affinity Using S-SIMS. *3.3.1. Interpretation of Positive Secondary Ion Mass Spectra.* Due to the use of a static regime, the mass spectra obtained with S-SIMS contain molecular information on the components in the uppermost monolayer of the analyzed sample. The assignment of structural ions to the analyzed compounds is crucial in mass spectrometry and deductive identification is desirable, yet there is still a lack of knowledge in this field. Different mechanisms of ion formation upon primary ion bombardment of surfaces have been proposed in the literature. The first of which, based on collision cascade theory, cannot explain the formation of large ions.[24] The so-called precursor model considers the presence of preformed ions in the solid prior to ion bombardment and therefore is only applicable to selected samples.[25] The model of Cooks and Busch[26] gives a description of the ion formation process based on a vaguely defined concept of energy isomerization, linking excitation of the solid by keV projectiles with ion formation in the selvedge, i.e., the dense gas phase above the sample. More recently, computer modeling has been used to reveal the sputtering and ion formation that governs S-SIMS.[27−31] Unfortunately, the

(24) Benninghoven, A.; Rüdenauer, F. G.; Werner, H. W. *Secondary ion mass spectrometry, chemical analysis*; John Wiley: New York, 1987; Vol. 86, pp 7−276.

(25) Benninghoven, A. *Ion Formation from Organic Solids (IFOS II), Springer Series in Chemical Physics 25*; Benninghoven, A., Ed.; Springer-Verlag: New York, 1983; pp 64−89.

(26) Cooks, R. G.; Busch, K. L. *Int. J. Mass Spectrom. Ion Phys.* **1983**, *53*, 111−124.

(27) Garrison, B. J.; Delcorte, A.; Zhigilei, L. V.; Itina, T. E.; Krantzman, K. D.; Yingling, Y. G.; McQuaw, C. M.; Smiley, E. J.; Winograd, N. *Appl. Surf. Sci.* **2003**, *203−204*, 69−71.

(28) Muramoto, T.; Yamamura, Y. *Appl. Surf. Sci.* **2003**, *203−204*, 143−147.

(29) Krantzman, K. D.; Postawa, Z.; Garrison, B. J.; Winograd, N.; Stuart, S. J.; Harrison, J. A. *Nucl. Instrum. Methods Phys. Res. B* **2001**, *180*, 159−163.

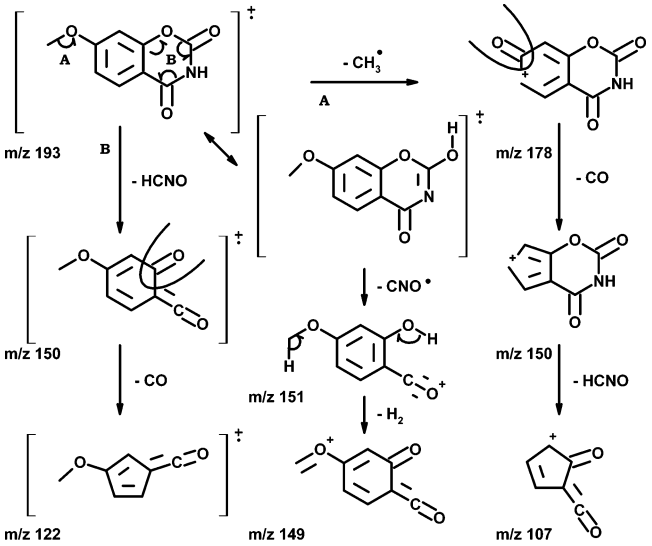

Figure 7. Tentative assignment of structural ions for MeO−BZD.

calculations are limited to the first few picoseconds of the ionization event, while the mass spectrum contains signals from the ion population generated in a nanosecond time domain. Furthermore, although sputtering events can be described accurately using molecular dynamics simulations, the difficulty to account correctly for the ionization step in the calculations prevents a direct link between experimental data and simulations.

Therefore, a purely empirical model, originally developed for laser microprobe mass spectrometry (LMMS), has been elaborated upon in our laboratory.[32−34] The so-called desorption−ionization (DI) model is derived from a large database of representative organic and inorganic compounds and appears applicable to both inorganic and organic S-SIMS results. In this model, the beam interaction with the solid is believed to create an energy gradient at the surface. Processes ranging from atomization to fast thermal desorption of intact thermolabiles occur. Subsequent ionization of desorbed neutrals takes place in the selvedge either by electron ionization (EI) or by adduct ionization (AI). In this way, ions with high and low internal energy, respectively, are produced. The fragments are primarily associated with the unimolecular decomposition of the radical molecular ions while adducts only undergo limited fragmentation by expulsion of small molecules. Finally, the characteristic features of the mass analyzer are explicitly used to link the ion population in the source to the finally detected ions.

To assess the affinity ranking of the different additives, adsorption was performed by dip coating Si wafers, covered with silver by sputter coating. Subsequent S-SIMS analysis revealed that the most relevant information has been available in the positive ion detection mode. Representative mass spectra of BZD, MeO−BZD, Me−BZD, BZTH, and BZTR adsorbed to silver are shown in Figure 6 for the *m*/*z* region between 110 and 420. Figure 7 shows the structural assignment of the ions of major diagnostic interest for MeO−BZD. The ionization and fragmentation mechanisms leading to structural assignment of the different ions have all been based on the DI model. The

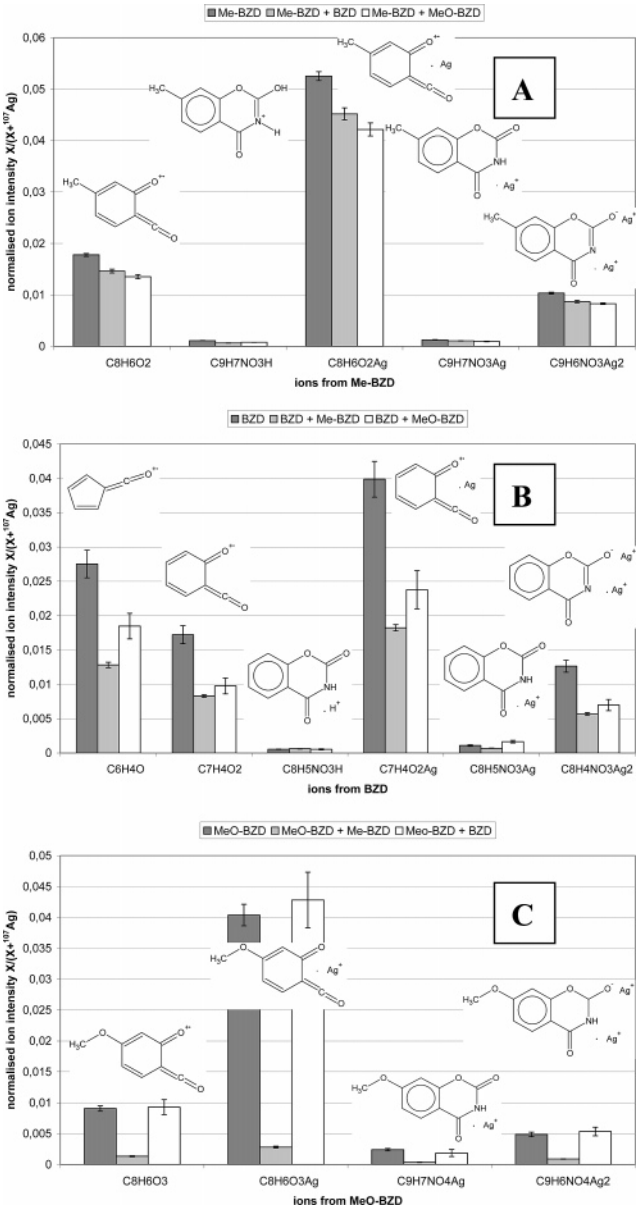

Figure 8. Normalized ion intensities measured for a Ag substrate dip-coated in a solution containing (A) Me−BZD (dark gray), Me−BZD with BZD (light gray) or with MeO−BZD (white); (B) BZD (dark gray), BZD with Me−BZD (light gray) or with MeO−BZD (white); (C) MeO−BZD (dark gray), MeO−BZD with Me−BZD (light gray), or with BZD (white).

obvious adducts of Ag^+ are not shown. The mass spectrum of Me−BZD is readily interpreted by applying identical fragmentation routes. The characteristic ions detected from compounds BZD, BZTH, and BZTR on Ag can be found elsewhere.[18] Apart from the consistency with the basic principles of organic mass spectrometry, the structural assignment is further supported by the *m*/*z* determination, the accuracy in TOF-S-SIMS being routinely better than 100 ppm. The combination of mass accuracy, likely formation mechanism, and structural assignment is given in detail in Tables A and B of the Supporting Information for Me−BZD and MeO−BZD, respectively.

Especially noteworthy is the detection of radical ions containing Ag for compounds BZD, Me−BZD, BZTH, and BZTR. For all but BZTH and MeO−BZD, $[M - H + Ag]^{+\bullet}$ is detected (although labels are omitted in Figure 6 because of overlap) while BZTH gives $[M - CS - H + Ag]^{+\bullet}$. Such ions must originate from EI of a species that has been desorbed as a neutral (or ion pair)

(30) Webb, R.; Chatzipanagiotou, A. *Nucl. Instrum. Methods Phys. Res. B* **2006**, *242*, 413−416.
(31) Harper, S.; Krantzman, K. D. *Appl. Surf. Sci.* **2004**, *231−232*, 44−47.
(32) Van Vaeck, L.; Claereboudt, J.; De Waele, J.; Esmans, E.; Gijbels, R. *Anal. Chem.* **1985**, *57*, 2944−2951.
(33) Van Vaeck, L.; Struyf, H.; Van Roy, W.; Adams, F. *Mass Spectrom. Rev.* **1994**, *13*, 189−208.
(34) Van Vaeck, L. *Encyclopaedia of analytical sciences, 2nd edition*; Worsfold, P., Thownsend, A., Poole, C., Eds.; Elsevier Ltd.: Oxford, UK, 2004; Vol. 1, pp 237−248.

Table 2. Summary of Comparing One-Component and Two-Component Solutions Dip-Coated on Ag Substrates[a]

	BZD	Me−BZD	MeO−BZD	BZTH	BZTR	argumentation on Ag affinity
BZD		↓	↓	⇊	⇊	others > BZD
Me−BZD	+/−		+/−	↓	⇊	BZTH, BZTR > Me−BZD > BZD, MeO−BZD
MeO−BZD	+/−	↓		⇊	⇊	BZTH, BZTR, Me−BZD > MeO−BZD > BZD
BZTH	+/−	+/−	+/−		↓	BZTR > BZTH > Me−BZD, MeO−BZD, BZD
BZTR	+/−	+/−	+/−	+/−		BZTR > others

[a] A decrease in ion intensity for the compound on the left when mixed with the given compound on top is symbolized by ↓, whereas +/− means that the ion intensities remain virtually constant.

and therefore exists as such in the solid before bombardment.[18] Otherwise stated, the corresponding molecules must have been adsorbed on the Ag substrate.

Finally, it must be mentioned that the information depth of typically one monolayer in S-SIMS results in the detection of many ions at low *m*/*z* primarily due to inevitable organic contamination of the sample surface. Furthermore, the spectra contain substrate-related ions such as Ag_n clusters ($n = 1$ at *m*/*z* 107−109, $n = 2$ at *m*/*z* 214−218, and $n = 3$ at *m*/*z* 321−327) and $Ag{\cdot}HCN{\cdot}H^+$ (*m*/*z* 135−137), $AgCN{\cdot}Ag^+$ (*m*/*z* 240−244), and $AgCl{\cdot}Ag^+$ (*m*/*z* 249−253). Additional signals such as $[C_6H_5Ag]^{+\bullet}$ (*m*/ *z* 184−186), $[C_6H_4Ag]^+$ (*m*/*z* 183−185), and $[C_6H_5Ag{\cdot}Ag]^+$ (*m*/*z* 291−295) are associated with nonspecific ions resulting from local pyrolysis.

3.3.2. Evaluation of Ion Intensities in Ag Affinity Studies. The Ag-coated Si wafers have been exposed to solutions containing either one or the different combinations of two additives. From the S-SIMS analysis of the different samples a comparison is made between intensities of characteristic ions for adsorptions from a one- or two-component system. The results are summarized in Figures 8A−C, giving the intensities of the characteristic peaks normalized to its sum with that of the $^{107}Ag^+$ ions.

At first view, the interpretation of these data may look rather tentative. Strictly speaking, relative affinity measurements imply that the surface has sufficient active sites, allowing each analyte to adsorb according to the specific equilibrium between the solution and the surface. In this case, the intensities recorded for the ions of one component should not decrease when another additive is present in the solution. Their adsorption behavior should not depend on each other. Competition implies that all active sites are already occupied by one additive. In this case, the presence of another adsorption candidate in the solution can only reduce the recorded ion intensities in comparison to the reference situation, where the solution contains only one additive.

Looking at the data for the system of BZD and Me−BZD, the change in intensities when the Me−BZD and the BZD are compared for the two-component and one-component solutions are given in Figures 8A and 8B, respectively. Specifically, the first two bars for the different Me−BZD-related ions in Figure 8A show that the presence of BZD in the solution does not affect the normalized intensities in comparison to the sample dip-coated in a solution of pure Me−BZD. In contrast, the first two bars in Figure 8B reveal that the presence of Me−BZD indeed leads to a decrease of the intensities recorded for the BZD specific ions. Hence, the data reflect relative affinity in conditions where also competitive effects or interactions occur. It has been shown that 1 h of dip coating is sufficient to reach the steady state and thereby limit the influence of kinetic effects on the measured intensities.[18]

Following this line of reasoning, the interpretation of the results becomes rather straightforward. Sometimes there is a discrepancy in the trends seen for the $[M - H + 2Ag]^+$ or $[M - H + Ag]^{+\bullet}$ ions on one hand and those of the $[M + H]^+$ or $[M + Ag]^+$ ions on the other. It has been reported[18] that the former ones must originate from chemisorbed species whereas the simple adduct can be formed by ion−molecule interactions in the selvedge. As a result, the former two ions deserve more attention during the interpretation of the Figures 8A−C. Comparison of plots for BZD, Me−BZD, and MeO−BZD in Figure 8A shows that for Me−BZD the same amount of species is adsorbed on the Ag substrate regardless of the presence of BZD or MeO−BZD in the solution. In contrast, Figure 8B shows that the amount of BZD adsorbed on Ag is strongly reduced by the presence of Me−BZD or MeO−BZD. Confirmation of this behavior can be found in Figure 8C, giving the ion intensities of MeO−BZD in the mixtures with Me−BZD and BZD. The intensities of the MeO−BZD specific ions stay virtually constant in the presence of BZD and the same behavior is seen for Me−BZD with BZD. Furthermore, MeO−BZD is barely found at the surface when exposed to a mixture with Me−BZD. The results for the BZTH ion intensities as a function of the composition of the solution are not explicitly shown as they are simple to describe. This additive seems to exhibit the highest affinity toward Ag. As a result, the intensities of the ions from BZTH remain nearly unchanged by the presence of a second additive in solution while ions from the other tone modifiers disappear when BZTH is added.

Finally, the stabilizer BZTR has also been tested in all combinations with the tone modifiers. In this case, it seems as if BZTR dominates the adsorption process and the intensities of the ions that are characteristic of the different tone modifiers almost vanish. As a result, these data have been omitted. The results for BZTH are in Figure D of the Supporting Information and show BZTR is apparently more hampered by Me−BZD, than by MeO−BZD, than by BZD.

The accompanying Table 2 summarizes the essential points from the discussion above and the corresponding affinity ranking to be deduced from the data in each "horizontal row". This set of equations looks internally consistent and can be converted to the following order. The highest silver affinity is seen for BZTR while that of BZTH still remains far superior to that of the other tone modifiers. The latter three show a further decrease in affinity for silver, starting from Me−BZD to MeO−BZD to BZD. As a result, the evaluation of the peak intensities of the structure characteristic ions in S-SIMS leads to the following affinity ranking: BZTR > BZTH > Me−BZD > MeO−BZD > BZD.

4. Conclusion

The study reports on the complementary use of UV−Vis spectrometry, SERS, and S-SIMS to obtain insight into the specific aspects of the behavior of tone modifiers and stabilizers in thermographic systems. Specifically, examination of silver affinities is of importance. To deal with the analytical complexity of the system, which is far beyond the current state of art of any technique, model systems have to be employed. Silver sols have been used for UV−Vis spectrometry and liquid SERS, while dry SERS analysis and S-SIMS have been applied to in-house developed SERS probes and sputter-coated silver substrates, respectively. All these methods and models have been used to

assess the relative affinity under conditions where competitive adsorption occurs by comparing the samples exposed or involving solutions containing one or two additives. Despite the differences in methods and samples, SERS analysis as well as S-SIMS provided evidence for the same ranking of 4 out of the 5 additives: BZTH > Me−BZD > MeO−BZD > BZD. This ranking can be rationalized on the basis of different SERS studies on other components and the "chemical hardness" of the hard and soft acids and bases (HSAB) theory. In ref 22 it is shown that the exocyclic sulfur in a compound analogous to BZTH (−COOH replaced by $-CH_3$) plays a pre-eminent role in the interaction of the molecule with Ag. Since sulfur yields a stronger interaction with Ag than nitrogen (assumingly being an important interaction center in BZD and derivatives),[9,35] the top place of BZTH in the ranking is not surprising. Due to only minor differences in the influence of the side chain on the nitrogen in BZD and derivatives, it is not appropriate to discuss the BZD series in this respect. A thorough investigation would be necessary to account for these differences but is beyond the scope of this manuscript.

The use of model systems may explain why the ordering of BZTR and BZTH according to SERS and S-SIMS is different. This might be due to the solvent used for sample preparation, namely, water with 1% methanol in SERS and 2-butanone in S-SIMS. Furthermore, the solvents must be completely removed for samples to be analyzed in S-SIMS unlike for those in SERS. The above-mentioned rationalization based on chemical hardness corresponds with the SERS ranking, not with that seen by S-SIMS. The reason might be that SERS is applied to samples containing water as solvent and the HSAB normally applies to this situation.

Summarizing, the complementariness of the different analysis techniques for this kind of research has been shown to yield interesting clues for a scientifically difficult issue like affinities. It gives scientific support to the empirical knowledge.

Acknowledgment. R.D.M. is indebted to the Institute for the promotion of innovation through science and technology in Flanders (IWT-Vlaanderen) for a Ph.D. grant. The authors also acknowledge support from the FWO, IUAP-V, and the EC NOE Nanobeams.

Supporting Information Available: Figure A shows the overlay of UV−Vis absorption spectra from silver hydrosols exposed to solutions containing two tone modifiers. Figure B shows the overlay of UV−Vis absorption spectra of silver hydrosols exposed to solutions of the stabilizer BZTR with every one of the four tone modifiers. Figure C shows the SER spectra obtained from a dedicated SERS probe after deposition of droplets of the different two-component mixtures. Figure D shows the normalized ion intensities of BZTR-specific ions measured for a Ag substrate dip-coated in a solution containing only BZTR or BZTR with BZD, MeO−BZD, or Me−BZD. Tables A and B show the ion structures with mass accuracies and formation pathways for Me−BZD and MeO−BZD, respectively. This material is available free of charge via the Internet at http://pubs.acs.org.

LA061591V

(35) Pearson, R. G. *Chemical Hardness*; Wiley-VCH: Weinheim, Germany, 1997; p 2.